RSC Advances

PAPER

View Article Online
View Journal | View Issue

Cite this: *RSC Adv.*, 2021, **11**, 28126

Post synthetically modified IRMOF-3 for efficient recovery and selective sensing of U(VI) from aqueous medium†

V. Venkata Sravani,[ab] Sarita Tripathi,[ab] B. Sreenivasulu,*[b] Satendra Kumar,[b] S. Maji,[b] C. V. S. Brahmmananda Rao,[ab] A. Suresh*[ab] and N. Sivaraman[ab]

A simple and efficient route to develop various novel functionalized MOF materials for rapid and excellent recovery of U(VI) from aqueous medium, along with selective sensing has been demonstrated in the present study. In this connection, a set of four distinct post synthetically modified (PSM) iso-reticular metal organic frameworks were synthesized from IRMOF-3 namely, IRMOF-PC (2-pyridine carboxaldehyde), IRMOF-GA (glutaric anhydride), IRMOF-SMA (sulfamic acid), and IRMOF-DPC (diphenylphosphonic chloride) for the recovery and sensing of U(VI) from aqueous medium. The MOFs were characterized by Fourier transform infrared spectroscopy (FTIR), powder XRD, BET surface area analysis, thermogravimetric analysis (TGA), NMR (^{13}C, ^{1}H and ^{31}P), Scanning Electron Microscopy (SEM), and energy dispersive X-ray spectroscopy (EDX). Among all MOFs, post synthetically modified IRMOF-SMA showed enhanced thermal stability of about 420 °C. The MOFs were investigated for U(VI) sorption studies using a batch technique. All the MOFs exhibit excellent sorption capacity towards U(VI) (>90%) and maximum uptake was observed at pH 6. Sorption capacity of MOFs have the following order; IRMOF-3-DPC (300 mg U g^{-1}) > IRMOF-SMA (292 mg U g^{-1}) > IRMOF-PC (289 mg U g^{-1}) > IRMOF-GA (280 mg U g^{-1}) > IRMOF-3 (273 mg U g^{-1}). IRMOF-DPC shows rapid sorption of uranium within 5 min with excellent uptake of U(VI) (>99%). The desorption of U(VI) was examined with different eluents and 0.01 M HNO_3 was found to be most effective. The fluorescence sensing studies of U(VI) *via* IRMOF-3 and its PSM MOFs revealed high sensitivity and selectivity towards U(VI) over other competing rare earth metal ions (La^{3+}, Ce^{4+}, Sm^{3+}, Nd^{3+}, Gd^{3+}, and Eu^{3+}), wherein IRMOF-GA displayed an impressive detection limit of 0.36 mg L^{-1} for U(VI).

Received 16th April 2021
Accepted 12th August 2021

DOI: 10.1039/d1ra02971a

rsc.li/rsc-advances

1. Introduction

Uranium is a widely employed fuel material in the nuclear industry as well as being a highly toxic element in the environment. The availability of uranium in the earth's crust and sea water is ~2.8 ppm and ~3.3 ppb, respectively.[1–3] There is a demand for alternative energy sources due to the rapid increase in population.[4] Among all energy sources, nuclear power is best for its extreme power density and is not harmful to the environment. Over the past few years, an appreciable amount of uranium in a highly stable form has seeped into the environment and ground water, due to various developmental activities including uranium mining, milling *etc.*[5–7] The release of uranium into ecosystems is highly undesirable. Hence uranium monitoring and regulations are crucial and also for preventing its accumulation. Hence there is a need to develop suitable materials for the efficient detection and removal of U(VI) from aqueous media.

A variety of chemical methods have been employed for the extraction of U(VI) from aqueous medium such as solvent extraction,[8] co-precipitation,[9] ion exchange,[10] adsorption,[11,12] and flotation.[13] Among all the techniques, adsorption is an effective and attractive technique for the removal of U(VI) from aqueous medium with trace quantities of uranium because of its low cost, ease of operation and high efficiency.[14,15] Although several conventional adsorbents such as zeolites,[16] activated carbon,[17] metal oxides,[12] and silica gels[18] are used for uranium extraction, these have limitations such as very low surface area, lower pore size, low adsorption efficiency, and less regeneration ability. Considering these limitations, it is important to develop novel materials for better and selective adsorption of U(VI) from aqueous medium.

Metal–organic frameworks (MOFs) are highly porous crystalline coordination polymers possessing properties such as high surface area, high porosity, tunable pore size, well ordered crystalline structure, magnetic property, and luminescence

[a]*Homi Bhabha National Institute, Indira Gandhi Centre for Atomic Research, Kalpakkam 603102, Tamil Nadu, India*

[b]*Material Chemistry and Metal Fuel Cycle Group, Indira Gandhi Centre for Atomic Research, Kalpakkam-603 102, Tamil Nadu, India. E-mail: bsrinu@igcar.gov.in; asu@igcar.gov.in; Tel: +91 44 27480500, ext. 24028*

† Electronic supplementary information (ESI) available. See DOI: 10.1039/d1ra02971a

properties.[19,20] MOFs exhibit various applications including gas adsorption/storage,[21–23] catalysis,[24,25] magnetism,[26] drug delivery,[27] membranes,[28] and sensing.[29–32] In addition, they are very prominent solid phase extractants (SPE) compared to conventional adsorbents because of the mild synthetic procedures, very high surface area (~14 000 m^2 g^{-1}), high and tunable pore size.

By adopting post synthetic modification (PSM) strategies, various organic functional groups can be grafted onto pristine MOFs to convert them to better materials with different physical and chemical properties without affecting the structural topology.[33–35] Although, different approaches exist in PSM strategy, covalent bond linker (organic ligand) modification is considered to be the best approach to prepare various functionalised MOFs for desired applications.[36,37] It is possible to prepare various permutations of MOFs *via* covalent grafting of organic ligand moieties (linker) to achieve desired utilities, by systematic procedures. PSM strategy also enables the synthesis of MOFs with enhanced structural stability.[38] The presence of pendant amino in MOFs is an excellent site for modification with desired organic functional groups by PSM strategies offering different applications *viz.*, catalysis, adsorption, and magnetism.[39,40] Gascon *et al.* reported PSM of amino pendant group in IRMOF-3 for catalytic applications.[41] While Cohen *et al.* reported PSM strategy on the modification of the UiO-66 amino group.[42,43] Therefore, by using PSM strategy various organic functionalities (hard bases) can be incorporated in the pristine MOF to get the efficient extraction of U(VI) (hard acid) from aqueous medium.[44]

In the last few years, iso-reticular metal–organic framework-3 (IRMOF-3) has been widely used for various applications such as heterogeneous catalysis,[45] gas storage/separation,[46] membranes,[47] and sensing of various metal ions,[48] due to its high surface area (BET reports 2200 m^2 g^{-1}), stability towards atmosphere, high temperatures (~400 °C) and its high luminescence property. Recently, the work carried out in our laboratory revealed the utility of PSM UiO-66-NH_2 grafted with various functionalities for extraction of U(VI) from the aqueous medium.[49] Additionally, various luminescent MOFs were constructed using Zn and lanthanides as metal nodes for sensing various metal ions,[50] nitro explosives,[51] and gases.[52] The successful studies on PSM of amino-pendant MOFs and the properties such as high surface area, extra stability, high porosity and highly luminescence, exhibited by IRMOF-3, motivated us to perform the sorption and sensing studies of U(VI) present in aqueous solution using different functionalised IRMOF-3 MOFs, for MOF with better efficiency in extraction and selectivity in sensing.

In the present study, we report the successful synthesis of four PSM MOFs belonging to IRMOF-3 category by covalent approach PSM at the amino pendant on IRMOF-3. The successful functionalization of IRMOF-3 MOFs was confirmed by FTIR, powder XRD, BET surface area analysis, TGA, ^{13}C and ^{1}H-NMR, and SEM & EDX. Sorption studies for U(VI) were carried out with IRMOF-3 and its PSM MOFs in the pH range of 2 to 9 and saturation sorption time also confirmed with kinetic studies. Excellent (97%) desorption of U(VI) sorbed on the MOFs was shown by 0.01 M HNO_3. IRMOF-3 and its PSM MOFs were also probed for their selectivity in sensing of U(VI), in the presence of competing metal ions (La^{3+}, Ce^{4+}, Sm^{3+}, Nd^{3+}, Gd^{3+}, and Eu^{3+}) in aqueous medium by fluorescence studies.

2. Experimental section

2.1 Chemicals and reagents

All the reagents, chemicals, and solvents used in the present study are commercial products and were used without any further purification. 2-Pyridine carboxylaldehyde, diphenylphosphonic chloride, glutaric anhydride, and 2-amino benzene dicarboxylic acid, *N*,*N*-dimethylformamide (DMF), triethylamine, acetonitrile, and dichloromethane (DCM) were procured from Merck. $Zn(NO_3)_2 \cdot 6H_2O$ was obtained from Acros organics, sulfamic acid was acquired from Loba Chemie Pvt. Ltd. Methanol and ethanol were procured from SD Fine-Chem Ltd and Changshu Hongsheng Fine Chemicals Ltd, respectively. U(VI) stock solution was prepared by dissolving appropriate amounts of uranyl nitrate hexahydrate ($UO_2(NO_3)_2 \cdot 6H_2O$) (Nuclear fuel complex, Hyderabad, India) in de-ionized water.

2.2 Synthesis of IRMOF-3

IRMOF-3 was synthesised as per the procedure reported by Gascon *et al.*,[41] with minor modifications. Herein, zinc(II) nitrate hexahydrate (4.5 g; 15 mmol) and 2-amino terephthalic acid (0.905 g; 5 mmol) were dissolved in DMF (50 mL) in a round bottom flask and stirred for 10 min. The solution mixture was poured into an autoclave and kept in an oven at 120 °C, for 24 h. This was then allowed to cool to room temperature, which resulted in the formation of light-yellow crystals. The synthesized IRMOF-3 was soaked in DCM for 3 days and every 12 h replaced with fresh DCM to remove entrapped DMF from the lattice, followed by drying at 100 °C for 24 h. The yield of IRMOF-3 obtained by this method was about 62% (3.2 g). The schematic diagram of the PSM MOFs synthesized from parent IRMOF-3 is shown in Scheme 1.

2.3 PSM of IRMOF-3

2.3.1 IRMOF-PC. The synthesis of IRMOF-PC was carried out as reported by Yaghi *et al.*[54] developed for $(Zn_4O)_3(BDC\text{-}NH_2)_3(BTB)_4$, with slight modifications mentioned by Sarita *et al.*[49] The percentage yield of the obtained IRMOF-PC was 62%. IR (KBr, cm^{-1}): 3114 cm^{-1} (br), 2351 cm^{-1} (w), 1604 cm^{-1} (vs), 1551 cm^{-1} (s), 1385 cm^{-1} (s), 1245 cm^{-1} (m), 1035 cm^{-1} (s), 768 cm^{-1} (m), 568 cm^{-1} (w).

2.3.2 IRMOF-GA. The synthesis was carried out by a procedure reported by Rassaei *et al.*[53] developed for NH_2-MIL-53 (Cr and Al) with slight changes mentioned by Sarita *et al.*[49] The percentage yield of the obtained IRMOF-GA was 50%. IR (KBr, cm^{-1}): 3136 cm^{-1} (br), 1540 cm^{-1} (vs), 1700 cm^{-1} (w), 1405 cm^{-1} (m), 1298 cm^{-1} (w), 1319 cm^{-1} (w), 850 cm^{-1} (m), 766 cm^{-1} (m), 566 cm^{-1} (w).

2.3.3 IRMOF-3-SMA. The synthesis was carried out by following the literature procedure reported by Sarita *et al.*[49] developed for UIO-66-NH_2. The percentage of yield of the

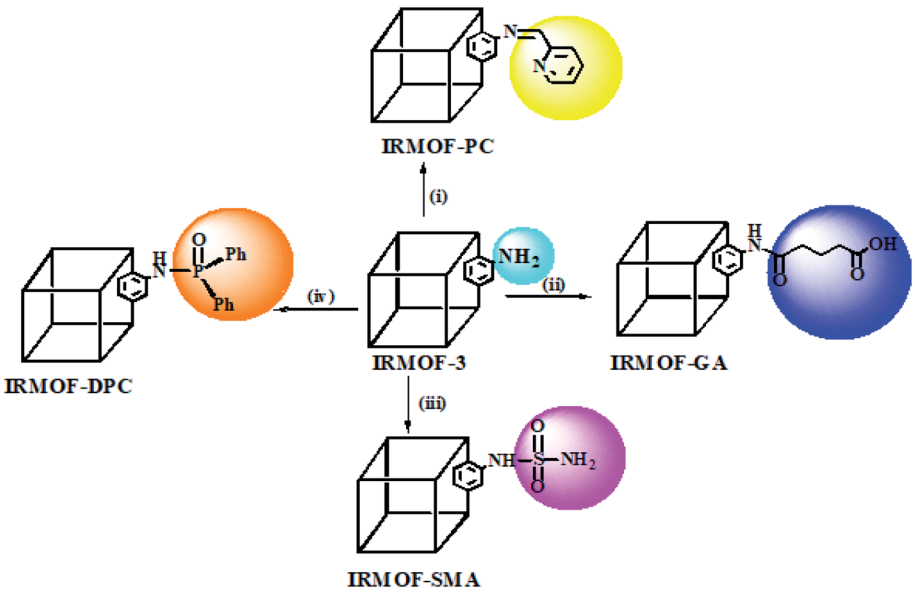

Scheme 1 PSM of IRMOF-3 with various functional groups: (i) 2-pyridine carboxaldehyde;[53] (ii) glutaric anhydride;[54] (iii) sulfamic acid;[49] (iv) diphenylphosphonic chloride.[55]

obtained IRMOF-SMA was 35%. IR (KBR, cm^{-1}): 3122 cm^{-1} (br), 1554 cm^{-1} (vs), 1434 cm^{-1} (w), 1395 cm^{-1} (s), 1312 cm^{-1} (m), 1243 cm^{-1} (m), 1129 cm^{-1} (w), 905 cm^{-1} (m), 842 cm^{-1} (m), 766 cm^{-1} (s), 573 cm^{-1} (w).

2.3.4 IRMOF-3-DPC. The synthesis was carried out by following the literature procedure by Freek *et al.*[55] was developed for NH_2-MIL-53(Al) by slight changes mentioned by Sarita *et al.*[49] The percentage yield of the obtained IRMOF-DPC was 93%. IR (KBR, cm^{-1}): 3396 cm^{-1} (br), 2337 cm^{-1} (w), 1678 cm^{-1} (m), 1501 cm^{-1} (s), 1422 cm^{-1} (m), 1310 cm^{-1} (w), 1230 cm^{-1} (vs), 1127 cm^{-1} (m), 963 cm^{-1} (w), 742 cm^{-1} (s), 534 cm^{-1} (w).

2.4 Characterizations

Fourier Transformed Infrared (FTIR) spectra (attenuated total reflection mode, 400–4000 cm^{-1}) for IRMOF-3 and its PSM MOFs were obtained using, a Bruker-Vertex 70 spectrometer, to confirm the presence of modified functional groups in PSM MOFs. Powder XRD data were acquired using GNR instrument with Cu Kα radiation (1.540598 Å) with a scan rate of 0.05° s^{-1} at 293 K to investigate the retained crystalline structure of the parent IRMOF-3 in all PSM MOFs. Thermo gravimetric analysis (TGA) was carried out using QMS 403 D NETZSCH in argon atmosphere, with a heating rate of 10 °C min^{-1} to measure the thermal stability of IRMOF-3 and PSM MOFs. BET surface area analysis was performed to obtain the surface area of MOFs on autosorb IQ station 1 at 77 K after pre-treatment by heating the samples under vacuum at 105 °C for about 24 h. NMR spectra obtained from a Bruker Avance DMX-400 spectrometer and operating frequencies are 400.13 MHz for ^{1}H-NMR, 100.61 MHz for ^{13}C-NMR, and 161.92 MHz for ^{31}P-NMR in DMSO-d_6 and HF. SEM analysis was done using SEM CARL ZEISS cross beam 340, and energy dispersive X-ray (EDX) data were obtained using EDX OXFORD instrument X-Max^N. Shimadzu Digital pH meter 335 was used to measure the pH of solutions. Shimadzu UV-3600 UV-Vis-NIR spectrophotometer was used to estimate U(VI) concentration. FLS920 model of spectrofluorimeter of Edinburgh instruments with a 450 W xenon lamp was used for fluorescence sensing studies of U(VI) from aqueous medium. Fused silica cuvette of 2 mm path length was used as the sample cell.

2.5 U(VI) sorption studies

U(VI) sorption studies from aqueous medium were carried out using IRMOF-3 and PSM MOFs by batch method. Studies were performed in the pH range 2 to 9 and pH was adjusted by adding small amounts of 0.1 or 3 M NaOH and 0.1 M HNO_3. For all sorption studies, U(VI) of given concentration, pH, contact time were optimized at room temperature (25 ± 1 °C). About 10 mg of MOF was equilibrated with 3 mL of uranyl nitrate solution (1000 mg L^{-1}) for 3 h in an equilibration tube at room temperature. Subsequently, the mixture was centrifuged for 10 min at 5000 rpm. The supernatant liquid was separated and used for the analysis of U(VI) using by UV-spectrophotometry using Arsenazo-III as the chromogenic agent (λ_{max} = 655 nm). For practical applications, the sorption rate of U(VI) from aqueous solution is associated with the evaluation of sorbents.

For all kinetic studies, 10 mg of the sorbent (MOF) was taken in 3 mL of U(VI) (1000 mg L^{-1}) at pH 5 and MOF solutions were kept for equilibration with varying time intervals from 0 min to 6 h followed by centrifugation for 10 min at 5000 rpm. The supernatant obtained after centrifugation was used for the uranium analysis. The sorption (%), distribution coefficient (K_d), and amount of uranium adsorbed (q_e) onto MOFs were calculated using the following equations:

$$\text{Sorption efficiency } (\%) = \frac{C_0 - C_e}{C_0} \times 100$$

$$K_d = \frac{C_0 - C_e}{C_e} \times \frac{V}{m}$$

$$q_e = \frac{C_0 - C_e}{m} \times V$$

Here, C_0 and C_e denote the initial and equilibrium concentrations (mg L^{-1}) of U(VI), V is the volume of solution (L) added, and m is the mass of sorbents (g). All the sorption experiments were performed in duplicate. The sorption efficiency (%), distribution coefficient (K_d), and amount of uranium adsorbed (q_e) were determined in duplicate. Reproducibility of data (sorption efficiency, K_d and q_e) and material balance was within ±5%, taking into consideration all other sources of errors including pipetting, weighing *etc.*

2.6 Desorption studies

Desorption studies were carried out to evaluate the recovery of the sorbed U(VI) from IRMOF-3 and its PSM MOFs. Initially, the U(VI) sorbed MOF samples were centrifuged for 10 min at 5000 rpm. The aqueous supernatant was decanted completely and sludge was used for desorption studies after drying at 100 °C. Desorption studies were performed using different eluents namely; 0.1 M HNO_3, 0.1 M Na_2CO_3, 0.01 M HNO_3, 0.01 M Na_2CO_3, and de-ionized water. The dried MOF samples were suspended in 3 mL of each eluent solution and equilibrated for 3 h followed by centrifugation for 10 min at 5000 rpm. The supernatant was analyzed for the concentration of U(VI) by UV-spectrophotometry.

Desorption (%) was calculated using the following equation:

$$\text{Desorption (\%)} = 100 - \left(\frac{\text{amount of U(VI) present in MOF} - \text{amount of U(VI) present the eluent}}{\text{amount of U(VI) present in MOF}} \times 100\right)$$

2.7 Recyclability studies

The reusability of IRMOF-3 and its PSM sorbents for U(VI) sorption were examined by performing recyclability tests. Foremost, the recovery of U(VI) from MOFs surface was executed by following the same procedure mentioned for desorption studies and the supernatant was analyzed for U(VI) concentration. After that, the MOF solutions were thoroughly washed with distilled water and dried at 100 °C following which the MOFs residue can be reused for sorption studies. The procedure was repeated twice for U(VI) sorption using MOFs.

2.8 Fluorometric analysis of U(VI)

Sensing U(VI) from aqueous medium using IRMOF-3 and its PSM MOFs at room temperature (25 °C) was analyzed from fluorescence spectra. Initially, 10 mg of finely ground MOFs were suspended in 25 mL of de-ionized water followed by sonication for 10 min for homogeneous distribution. Various concentrations of U(VI) solution (0 to 300 mg L^{-1}) at pH 4 were prepared from 1000 mg L^{-1} of U(VI) stock solution. Each test sample was prepared by mixing 250 μL of MOF suspension, varying concentrations of U(VI) solution, 10 μL of 0.5 M $NaNO_3$, and remaining portion made up to 500 μL with ultra-pure water (pH 4). The purpose of adding $NaNO_3$ is to fix the nitrate ions concentration same in all the solution. Therefore, quenching of fluorescence intensity for all the MOFs is only due to U(VI). The test solutions were aged for 2 h, followed by fluorimetric analysis.

In order to investigate the selectivity of IRMOF-3 and its PSM MOFs towards U(VI) from aqueous medium, 1000 mg L^{-1} solutions of various lanthanide ions (La^{3+}, Ce^{4+}, Nd^{3+}, Sm^{3+}, Gd^{3+}, and Eu^{3+}) were prepared at pH 4. The fluorimetric sensing studies of U(VI) with competing metal ions were carried out in the similar way of mentioned for U(VI) by considering 100 mg L^{-1} as standard concentration. In order to minimize the uncertainty due to suspension change and instrumental fluctuations, all spectra were recorded in duplicate.

3. Results and discussion

The pendant amino group present in IRMOF-3 was used for the synthesis of four functionalised MOFs namely IRMOF-PC, IRMOF-GA, IRMOF-SMA, and IRMOF-DPC using 2-pyridine carboxylaldehyde, glutaric anhydride, sulfamic acid, and di phenyl phosphonic chloride, respectively by PSM strategy. The newly synthesised PSM MOFs exhibited varied properties *viz.* stability, surface area, pore size, and binding efficiency towards U(VI).

The synthesised IRMOF-PC having the imine (C=N) group furnishes metal binding site obtained by covalent grafting of 2-pyridine carboxaldehyde onto IRMOF-3. The presence of amide (NH–CO–) and carboxylic acid (–COOH) groups simultaneously cannot be achieved by direct synthesis, but through PSM by treating IRMOF-3 with glutaric anhydride resulted into IRMOF-GA possessing both the functional groups offering more binding efficiency. The sulphur functionalised MOFs (S-MOFs) have been extensively studied as solid phase extractants towards adsorption of heavy metals (Hg(II), Pb(II), Cd(II)), following HSAB principle.[56] Therefore, IRMOF-SMA was synthesised by treating IRMOF-3 with sulfamic acid *via* PSM strategy in order to analyse the behaviour of sulphur based extractant for U(VI) from aqueous medium. Phosphorous based functional groups are widely used for the extraction of radionuclides *e.g.*, solvent extraction using some alkyl phosphates. This motivated us to synthesize phosphorous based, IRMOF-

DPC, by treating IRMOF-3 with di phenyl phosphonic chloride and studied for extraction of U(VI).

3.1 Characterization

The IR spectrum of synthesised IRMOF-3 was verified and matched well with reports, confirming the formation of IRMOF-3. The IR spectra of PSM MOFs confirmed the presence of grafted functional groups (Fig. S1†). Compared to the parent IRMOF-3, the representative IR peak for C=N in IRMOF-PC is observed at 1604 cm^{-1}, a medium intense peak observed at about *ca.* 1700 cm^{-1} (NH–CO–) may be attributed to the amide functional group present in IRMOF-GA, the strong peak observed at 1225 cm^{-1} indicates the presence of (S=O) in IRMOF-SMA, and strong intense peak observed at 1127 cm^{-1} is attributed to (P=O) in IRMOF-DPC. The IR results confirm the successful synthesis of different functionalized IRMOF-3 MOFs *via* PSM strategy.

The powder XRD patterns of synthesized IRMOF-3 matched well with reported patterns, confirming its formation (Fig. S2†). The PSM MOFs exhibit PXRD patterns similar to that of parent IRMOF-3 indicating intact structure of IRMOF-3, with no apparent loss of crystalline nature upon grafting of functional groups. Marginal changes observed, could be attributed to the variation in the electron density due to the presence of functional groups.

Thermogravimetric (TGA) profile for IRMOF-3 and its PSM MOFs are different due to the presence of different functional groups (Fig. S3†). The parent IRMOF-3 is stable up to 400 °C and is similar to the reported one. The TGA profile of IRMOF-PC showed that it is less stable than parent MOF and is stable up to 330 °C. TGA profile of IRMOF-GA and IRMOF-DPC are similar to the parent MOF and these are stable up to 400 °C and 360 °C respectively. Interestingly, thermal stability of IRMOF-SMA is high and it is stable up to 420 °C. However, all the four PSM MOFs are having the good thermal stability (>300 °C).

The PSM of IRMOF-3 was further confirmed by acid-digested (HF and DMSO-d_6) NMR spectroscopy (^{1}H-, ^{13}C- and ^{31}P-NMR). The ^{1}H-NMR spectra of all PSM MOFs exhibit a down field shift for the modified BDC ligand, compared to the parent MOF, along with the unmodified ones (Fig. 1). Additionally, IRMOF-GA displayed new peaks corresponding to the alkyl groups of glutaric anhydride appearing in the range of 1.4–2.5 ppm. IRMOF-PC and IRMOF-DPC exhibit peaks in the aromatic region and can be attributed to the iminopyridine moiety and aromatic protons of the new phenyl rings, respectively. The ^{13}C-NMR spectra also exhibit new peaks corresponding to the modified frameworks and confirm the presence of intended functionalities in the framework (Fig. S4†). In addition, the ^{31}P-NMR spectrum of IRMOF-DPC is simulated with that of the starting material, *i.e.*, diphenylphosphinic chloride (Fig. S5†). Therefore, the NMR studies confirm the conversion of IRMOF-3 to modified MOFs.

The surface morphology and quantitative compositional characterization of synthesized IRMOF-3 and obtained PSM MOFs were done by SEM and EDX analysis, respectively (Fig. S6–S10†).

BET surface area analysis was performed using approximately 0.8–1 g of MOFs in order to observe the changes in surface area as well as porosity by measuring the Brunauer–Emmett–Teller (BET) with N_2 at 77 K (Table S2†). The results reveal that decrease in the porosity and surface area for functionalised MOFs due to the presence of various grafted organic functional groups. The large functional groups were filled in the pores led to decrease in size and followed by decrease in porosity.

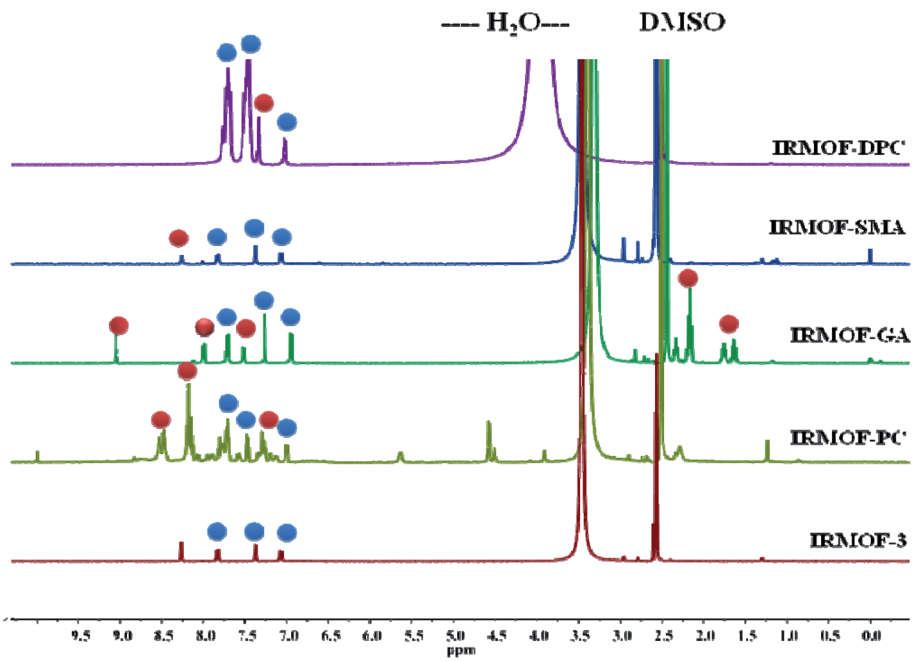

Fig. 1 ^{1}H-NMR (400 MHz, in DMSO-d_6) spectra of IRMOF-3 and its functionalized MOFs.

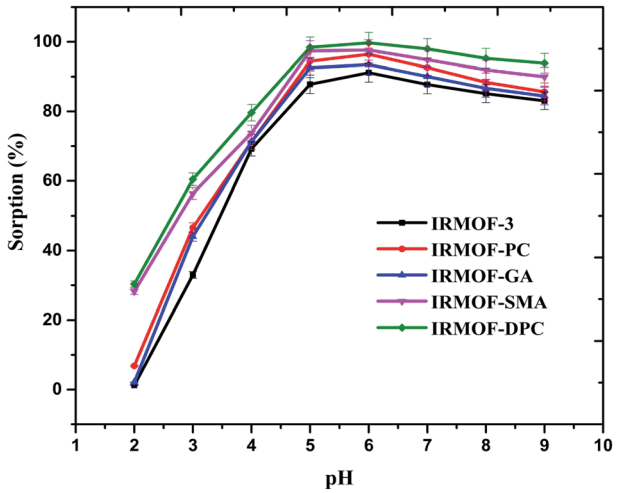

Fig. 2 Effect of solution pH on U(VI) sorption (%) onto IRMOF-3 and its PSM MOFs, $t = 180$ min, $m_{sorbent} = 10.0$ mg, $V_{solution} = 3$ mL, $C_0 = 1$ mg mL^{-1}, $T = 25 \pm 1$ °C.

3.2 U(VI) sorption studies

In order to compare the U(VI) sorption behaviour of the newly synthesized PSM MOFs and the parent IRMOF-3, a series of batch experiments were performed at various conditions of pH, contact time, and U(VI) of known concentration.

3.2.1 Effect of solution pH on sorption behaviour of U(VI). The pH of the solution plays a very crucial role in sorption of U(VI) from aqueous (acidic/basic/neutral) medium, since it affects the specific state of uranium as well as the surface charge distribution of binding sites across sorbents. In order to investigate the influence of solution pH on the sorption behaviour of U(VI) onto IRMOF-3 and its PSM MOFs, studies were performed as a function of the pH of the solution in the range from 2 to 9 (Fig. 2). The results revealed that the sorption of U(VI) strongly depends on pH. Sorption of U(VI) onto MOFs is less up to pH 4 beyond which sorption of U(VI) increases up to pH 6 for all MOFs and then decreases after pH 7. The modified IRMOF-DPC exhibits greater sorption behaviour (300 mg U g^{-1}) than that of IRMOF-3 (239 mg U g^{-1}). The increasing order of sorption capacity of U(VI) onto IRMOF-3 and PSM MOFs (Table 1) are as follows: IRMOF-3-DPC (300 mg U g^{-1}) > IRMOF-SMA (292 mg U g^{-1}) > IRMOF-PC (289 mg U g^{-1}) > IRMOF-GA (280 mg U g^{-1}) > IRMOF-3 (273 mg U g^{-1}). Sorption (%) of IRMOF-3 and its PSM MOFs at pH 6 is shown in Fig. 3.

The effect of solution pH on U(VI) sorption by IRMOF-DPC is shown in Fig. 4 for more clarity. The improved sorption behaviour shown by IRMOF-DPC could be is due to the strong

Table 1 Sorption of U(VI) onto IRMOF-3 and PSM MOFs (pH = 6)

MOF	Sorption (%)	K_d	q_e (mg g^{-1})
IRMOF-3	91 ± 2.7	3096 ± 93	273 ± 8
IRMOF-PC	96 ± 2.9	8122 ± 244	289 ± 8
IRMOF-GA	93 ± 2.8	4277 ± 128	280 ± 9
IRMOF-SMA	97 ± 2.9	12 384 ± 371	292 ± 9
IRMOF-DPC	99 ± 3.0	24 983 ± 749	300 ± 9

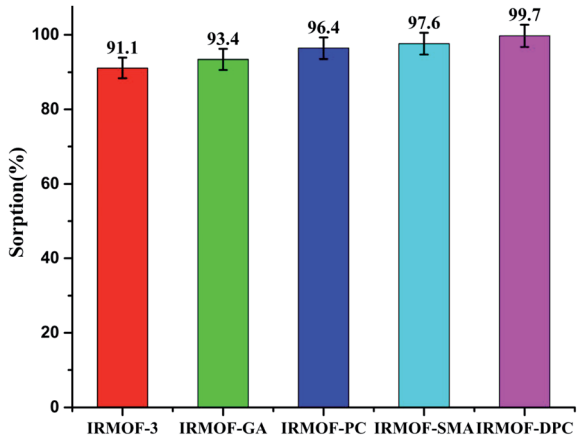

Fig. 3 U(VI) sorption (%) onto IRMOF-3 and its PSM MOFs; pH = 6, t = 180 min, $m_{sorbent} = 10.0$ mg, $V_{solution} = 3$ mL, $C_0 = 1$ mg mL^{-1}, $T = 25 \pm 1$ °C.

electrostatic interaction between hard Lewis acid U(VI) and hard Lewis base: phosphoryl oxygen (P=O). Furthermore, the bonding between IRMOF-DPC and U(VI) was confirmed by FTIR (Fig. 5) wherein the intensity of P=O (1127 cm^{-1}) decreases significantly with a peak shift due to bonding with U(VI). Additionally, the new intense strong sharp peak observed at 925 cm^{-1} is attributed to the UO_2^{2+} ions. The IR analysis thereby confirms the formation of strong bond between P=O and U(VI).

Although all the five MOFs showed significant extraction efficiency towards U(VI) from aqueous medium, in terms of response time (~5 min) (Fig. 6a), thermal stability (400 °C) and sorption efficiency (99.1%), IRMOF-DPC is the best sorbent for the extraction of U(VI) from aqueous medium. The sorption (%), distribution coefficient (K_d), and amount of U(VI) sorbed (q_e) for all the MOFs are shown in Table 1.

3.2.2 Effect of contact time and sorption kinetics. The kinetic studies confirmed that IRMOF-DPC (Fig. 6a) responds

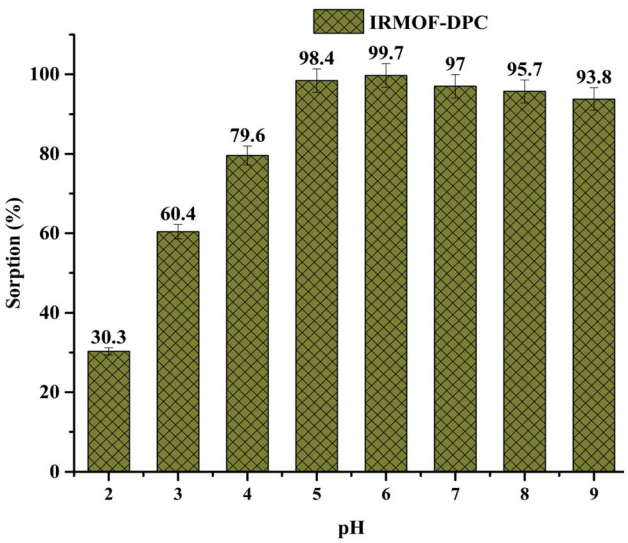

Fig. 4 Effect of solution pH (2 to 9) on U(VI) sorption (%) onto IRMOF-DPC, $t = 180$ min, $m_{sorbent} = 10.0$ mg, $V_{solution} = 3$ mL, $C_0 = 1$ mg mL^{-1}, $T = 25 \pm 1$ °C.

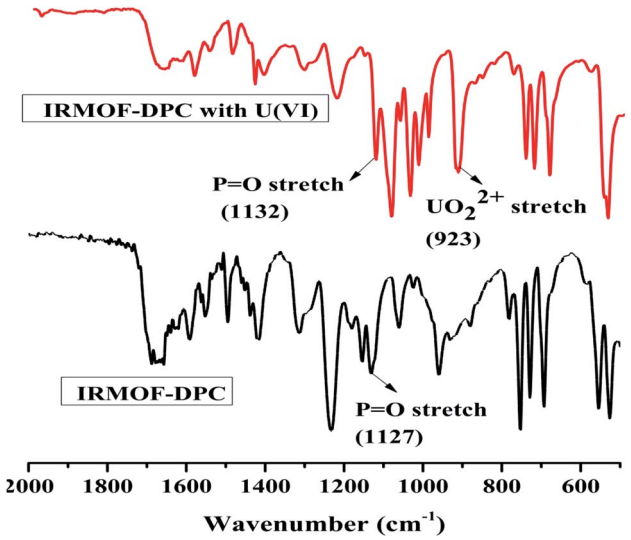

Fig. 5 FTIR spectra of IRMOF-DPC before and after U(VI) sorption.

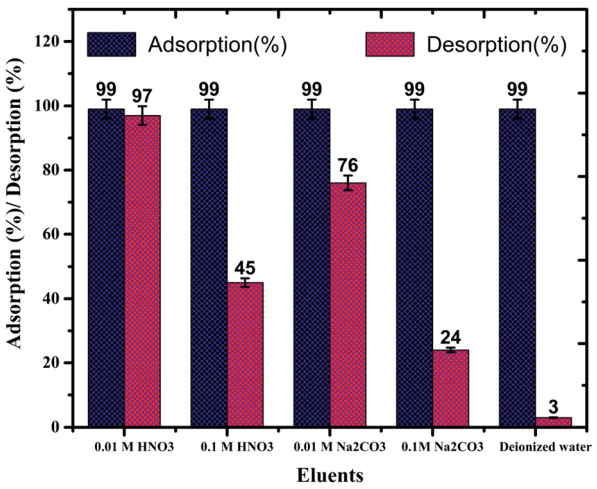

Fig. 7 Sorption (%)/desorption (%) bar graph of U(VI) from IRMOF-DPC.

quickly (~5 min) and has highest sorption efficiency towards U(VI) from aqueous medium. For IRMOF-3, IRMOF-PC, IRMOF-GA, and IRMOF-SMA the saturation sorption was observed after 3 h, however they exhibited higher efficiency beyond 60 minutes (Fig. S11†).

The plot drawn between contact time (t, min) *vs.* t/q_t (q_t is the amount of U(VI) sorbed at a time t) shows the straight line and it is not passing through origin indicating IRMOF-DPC follow pseudo second order kinetics (Fig. 6b) and all other MOFs also follow similar trend (Fig. S12†).

3.3 Desorption and recyclability studies

In order to recover the U(VI) from MOFs, a series of desorption studies were performed with different eluents (0.1 M HNO_3, 0.01 M HNO_3, 0.1 M Na_2CO_3, 0.01 M Na_2CO_3, and de-ionised water). The results revealed that 0.01 M HNO_3 (Fig. S13;† 97%) is an excellent desorbing agent for U(VI) sorbed on IRMOF-

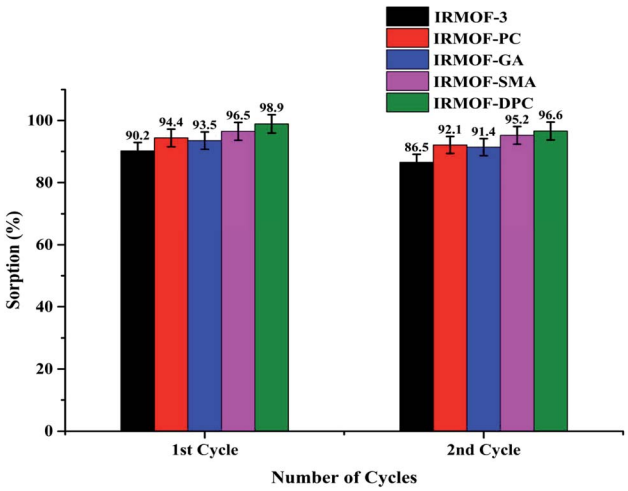

Fig. 8 Recyclability tests bar graph for IRMOF-3 and PSM MOFs.

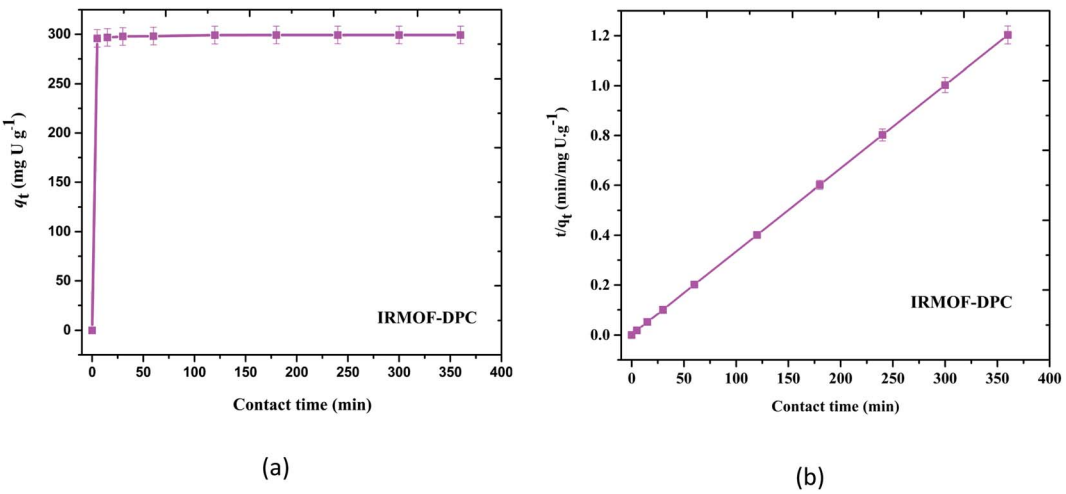

Fig. 6 Effect of contact time on (a) q_t and (b) t/q_t of U(VI) sorption onto IRMOF-DPC; pH = 6, $m_{sorbent}$ = 10.0 mg, $V_{solution}$ = 3 mL, C_0 = 1 mg mL^{-1}, $T = 25 \pm 1$ °C.

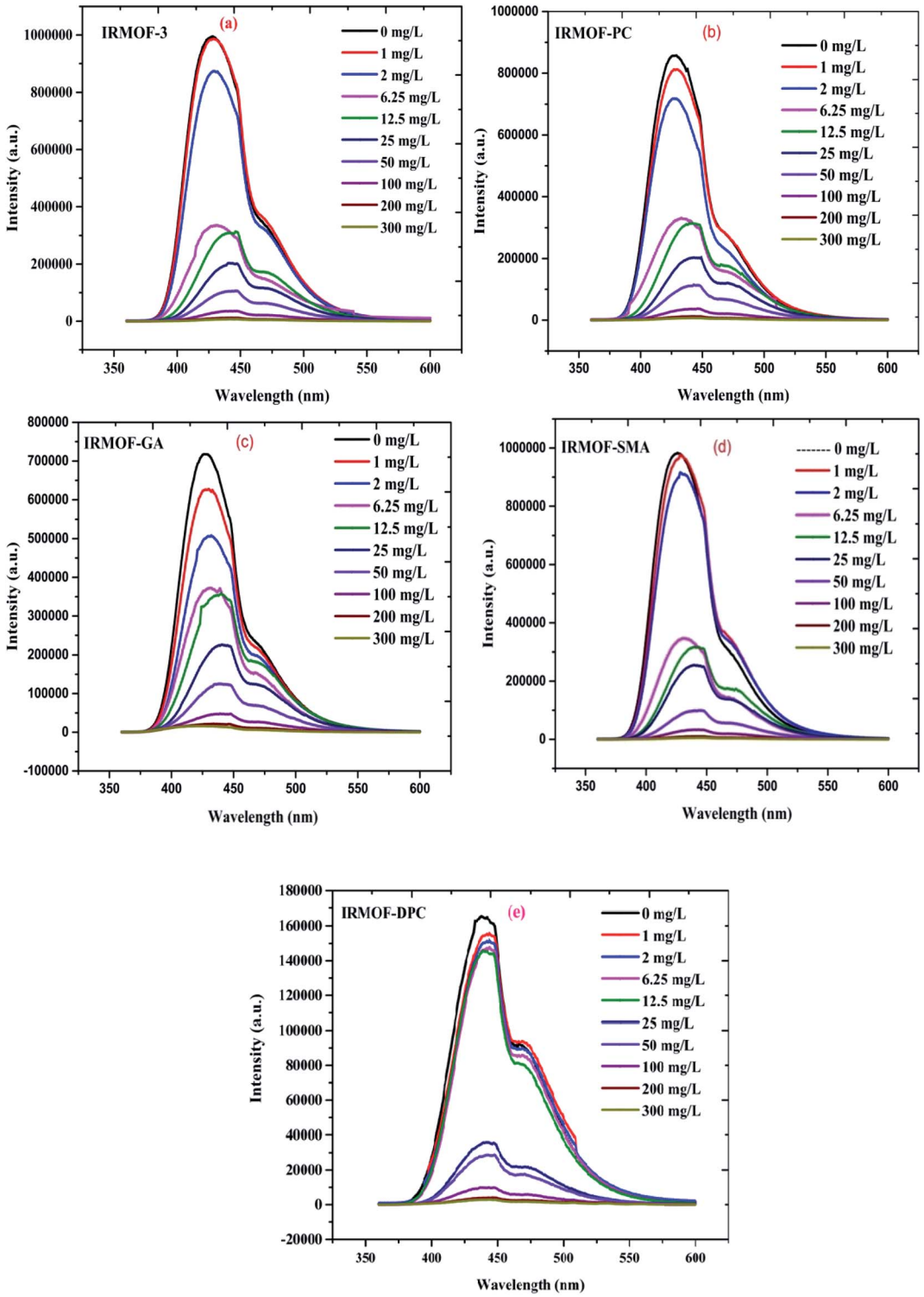

Fig. 9 The emission spectra of (a) IRMOF-3; (b) IRMOF-PC; (c) IRMOF-GA; (d) IRMOF-SMA; and (e) IRMOF-DPC with increasing U(VI) concentration (0 to 300 mg L^{-1}).

3 and its PSM MOFs. Using 0.01 M HNO_3 eluent up to 97% U(VI) was recovered from IRMOF-DPC (Fig. 7). Here, desorption (%) was calculating based on the amount of U(VI) sorbed on MOFs, and does not depend on the initial concentration of U(VI).

Recyclability studies were performed with IRMOF-3 and its PSM MOFs for U(VI) sorption in order to understand the reusability aspects of these MOFs for practical applications. Sorption (%) indicates only marginal decrease in sorption capacity for U(VI) after two cycles (Fig. 8). Therefore, IRMOF-3 and its PSM MOFs are versatile sorbents for reusability for extraction of U(VI) from aqueous medium.

3.4 U(VI) sensing studies

IRMOF-3 and its PSM MOFs were examined for fluorescence sensing of uranyl ions. The excitation wavelengths are different for different MOFs; IRMOF-3 (λ_{ex} = 428 nm), IRMOF-PC (λ_{ex} = 426 nm), IRMOF-GA (λ_{ex} = 330 nm), IRMOF-SMA (λ_{ex} = 424 nm), and IRMOF-DPC (λ_{ex} = 334 nm). The difference in wavelengths is due to the presence of different functional groups and variation in charge transfer from ligand to metallic node present in the MOFs. The fluorescence intensity of MOFs due to ligand-to-metal charge transfer (LMCT) spectra primarily depends on the presence of benzene derivatives in linkers, which plays a crucial role in the fluorescence intensity. Depending on the electronic

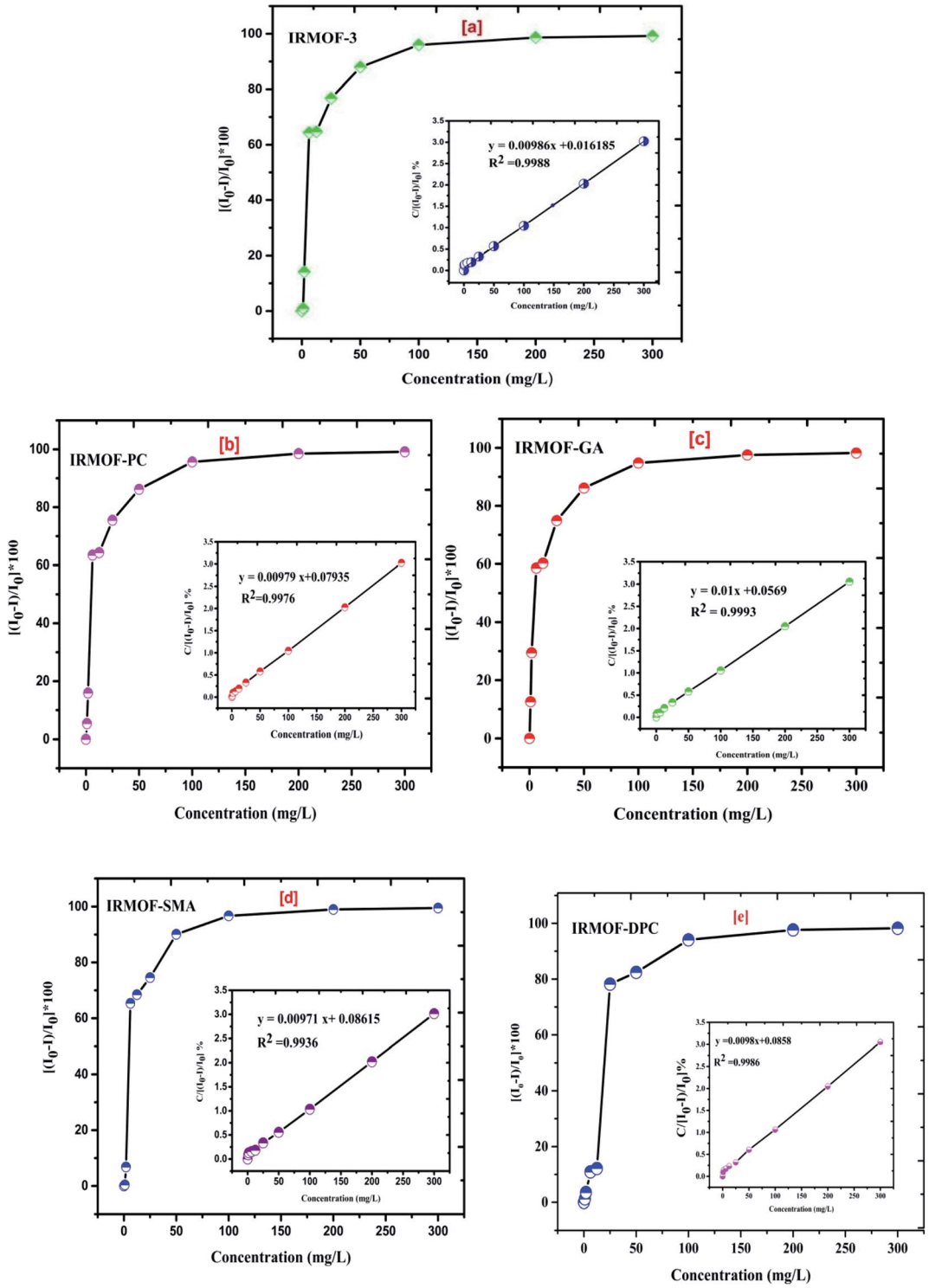

Fig. 10 The effect of increasing U(VI) concentration (0 to 300 mg L^{-1}) on quenching (%) of (a) IRMOF-3; (b) IRMOF-PC; (c) IRMOF-GA; (d) IRMOF-SMA; and (e) IRMOF-DPC.

configuration of metal and relative linker and metal orbital energies, the metal ion influences the emission. Initially, the charge transfer from the amino ($-NH_2$) substituted benzene rings to Zn-metal was very high in IRMOF-3 resulting in high fluorescence intensity. However, PSM MOFs displayed decreased fluorescence intensities due to grafted organic functional groups. Among them, IRMOF-DPC exhibits lowest fluorescence intensity, compared to IRMOF-3, and can be attributed to the presence of two aromatic rings which could hinder the ligand to metal charge transfer (LMCT).[57]

In order to understand the effect of U(VI) sorption on fluorescence intensity, IRMOF-3 and its PSM MOFs suspensions (250 μL) were treated with varied concentrations of U(VI) (1 to 300 mg L^{-1}) in ultra-pure water, at pH = 4. It can be seen (Fig. 9) that all the MOFs except IRMOF-DPC show good quenching when concentration of U(VI) is 6.25 mg L^{-1}. The quenching of fluorescence intensity of the MOFs at 6.25 mg L^{-1} of U(VI) shows the following trend: IRMOF-SMA (65.4%) > IRMOF-3 (64.3%) > IRMOF-PC (63.5%) > IRMOF-GA (58.6%) > IRMOF-DPC (10.9%). Further increase in U(VI) concentration (up to 300 mg L^{-1}), leads to further decrease in fluorescence intensity. Langmuir model was used here to fit the fluorescence quenching ratio [$((I_0 - I)/I_0) \times 100$] plotted as a function of uranium concentration. We hypothesize that the decrease in fluorescence intensities of

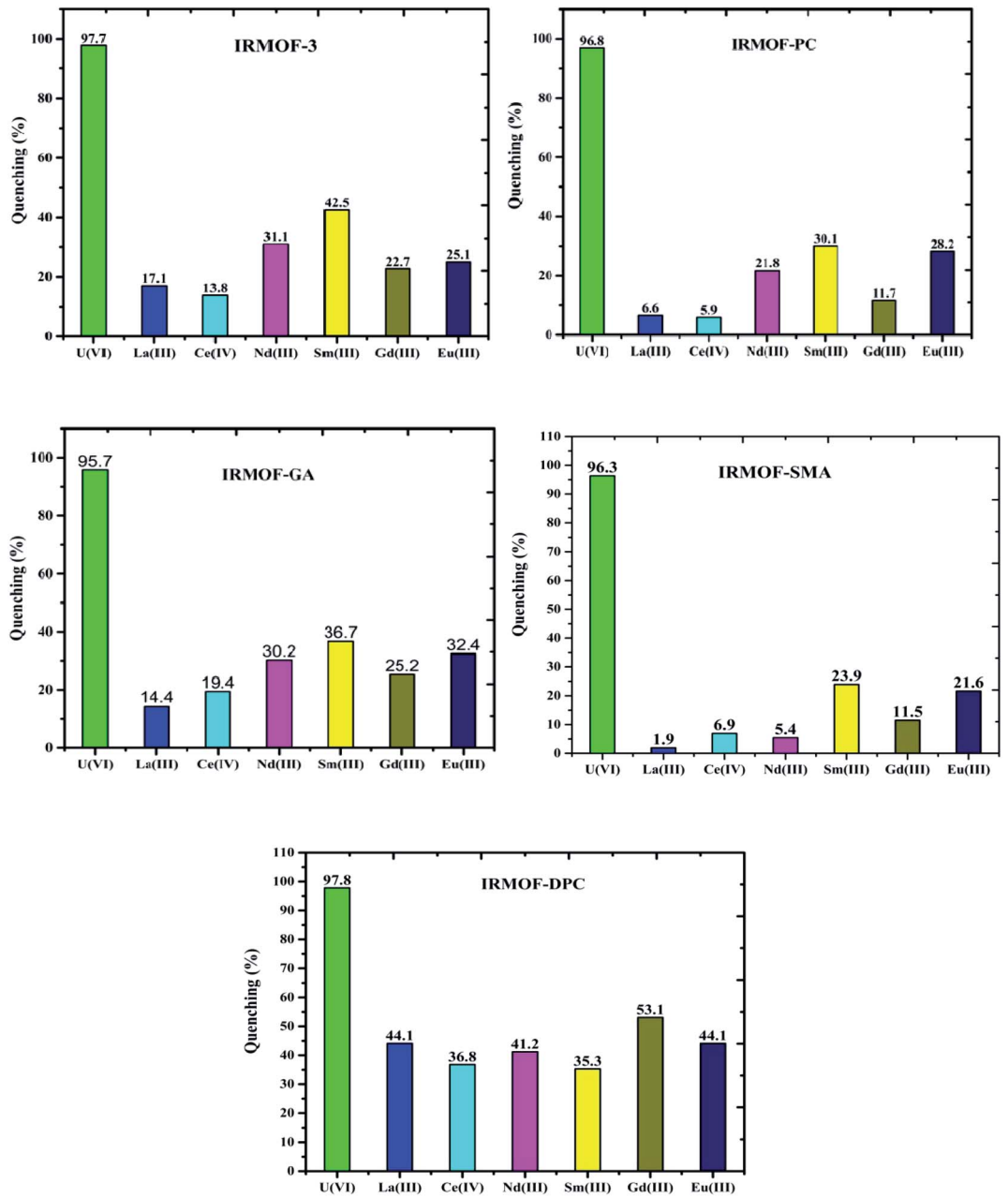

Fig. 11 Quenching (%) of IRMOF-3 and its PSM MOFs with U(VI) and competing metal ions (La^{3+}, Ce^{4+}, Nd^{3+}, Sm^{3+}, Gd^{3+}, and Eu^{3+}); concentration of each ion is 100 mg L^{-1}.

IRMOF-3 and its PSM MOFs following the interaction of ligands in MOFs with U(VI), was due to the variance in charge transfer from frameworks to U(VI). Therefore, the fluorescence quenching phenomena can be directly correlated with U(VI) concentration-dependent sorption behaviour on IRMOF-3 and its PSM MOFs, which is described by Langmuir model fitting (Table S4†). When the simulated Langmuir equation was transformed into the correlation between U(VI) concentration (C) and $C/[(I_0 - I)/I_0 \times 100]$ (Fig. 10 inset), a nearly linear correlation was obtained. The correlation coefficients of IRMOF-3 and its PSM MOFs using Langmuir model was found to be greater than 0.993 and are shown in Table S4.† Therefore, this method can be used for the quantitative analysis of uranium over a wide range of concentration (6.25 to 300 mg L^{-1}).

3.5 U(VI) detection limit and selectivity

Comparison of fluorescence intensity of PSM MOFs and parent MOF displayed significant quenching at and above 6.25 mg L^{-1} of U(VI) (Fig. 9). It can be seen that IRMOF-GA responded more sensitively to U(VI) than other MOFs. Even 1 mg L^{-1} of U(VI) quenches the fluorescence intensity of the MOF by nearly 30%. The detection limit (3σ/slope) was calculated to be 0.36 mg L^{-1}, clearly demonstrating the potential application of IRMOF-GA as quantitative sensor for U(VI). Xiohong *et al.*[58] already reported PtRu bimetallic based MOFs for U(VI) sensing with detection limit 0.024 μM and Linnan Li *et al.*[59] also reported U(VI) sensing with detection limit 0.9 μM. Although, the reported MOFs are showing the good detection limit for U(VI), by considering the quick response time (~5 min), easy synthesis, high extraction efficiency (300 mg g^{-1}) for U(VI) made these functionalised IRMOF-3 MOFs selective agents for U(VI) extraction and sensing.

In order to investigate the selective sensing of U(VI) over other metal ions from aqueous medium using IRMOF-3 and its PSM MOFs, lanthanide ions (La^{3+}, Ce^{4+}, Nd^{3+}, Sm^{3+}, Gd^{3+}, and Eu^{3+}) were chosen for fluorescence studies. The quenching of fluorescence intensity of all MOFs by lanthanides was found to be in the range of 2 to 53% for 100 mg L^{-1} of lanthanides (Fig. 11). However, it is to be noted that this quenching is lower than that of same amount of U(VI) (~98%) indicating that all MOFs were highly selective for sensing of uranyl ions. The selectivity could be due to the electrostatic interaction between U(VI) and varied functional groups present in MOFs, which leads to efficient energy transfer, by resonance, than the lanthanide ions. This effect can be further investigated by the soft nitrogen donor ligand (IRMOF-GA, amide group), which also enables selective enrichment of the U(VI) than lanthanide ions. Furthermore, the arrangement of coordination sites in the crystalline structures of MOFs contain variable donor groups namely amine (NH), imine (C=N), amide (NH–C=O), carboxylate (–COO), sulfamide (NH–S=O), phosphamide (NH–P=O) as preferential binding sites for the U(VI) ions over other competing metal ions. These results demonstrate that the excellent detection selectivity toward U(VI) may indeed originate from the capability of efficient and selective enrichment of U(VI) by IRMOF-3 and PSM MOFs, providing opportunities for applications in uranium sensing within aqueous media.

4. Conclusions

In the present study, we report four PSM MOFs namely, IRMOF-PC, IRMOF-GA, IRMOF-SMA, and IRMOF-DPC synthesised *via* covalent grafting of functional moieties (amide, anhydride, sulphur, and phosphorous) by modifying pendant amino ($-NH_2$) group present in the IRMOF-3. The resultant MOFs displayed varying porosity, surface area, stability, and binding affinities. These properties made PSM MOFs significance difference towards U(VI) sorption in aqueous medium (pH = 2 to 9), due to the different electrostatic interactions between grafted functional groups and U(VI). The leaching studies revealed that quantitative recovery of U(VI) from MOFs and good recyclability studies showed considerable stability of these MOFs making them suitable environmentally clean materials. Therefore, the easy functionalization of MOFs using PSM to get the selective sorbents becomes useful for sorption of U(VI) from aqueous medium.

Additionally, present study revealed that IRMOF-3 and PSM MOFs are excellent materials for the sensing and detection of U(VI) from aqueous medium. IRMOF-GA offered impressive detection limit (0.36 mg L^{-1}). These results revealed the participation of organic functional groups in the fluorescence sensing of U(VI). Moreover, these MOFs furnished excellent selectivity *via* fluorescence quenching for U(VI) (~98%) over other lanthanide ions (La^{3+}, Ce^{4+}, Nd^{3+}, Sm^{3+}, Gd^{3+}, and Eu^{3+}) (2–53%). This strategy is useful for studies seeking to synthesize highly stable solid-state sorbents and sensors selective to U(VI) from aqueous media, within the context of nuclear industry as well as the ecosystem.

Conflicts of interest

There are no conflicts to declare.

Acknowledgements

We are thankful to Dr N. Ramanathan for the FT-IR spectra, Mr Afijith Nair for powder XRD, Dr S. Balakrishnan for TGA, Mr Rakesh (VIT Vellore) for NMR spectra, and Dr Manish Chandra for SEM & EDX.

References

1 S. A. Abbasi, *Int. J. Environ. Anal. Chem.*, 1989, **36**, 163–172.
2 C. Falaise, C. Volkringer, R. Giovine, B. Prelot, M. Huve and T. Loiseau, *Dalton Trans.*, 2017, **46**, 12010–12014.
3 J. Park, R. T. Jeters, L.-J. Kuo, J. E. Strivens, G. A. Gill, N. J. Schlafer and G. T. Bonheyo, *Ind. Eng. Chem. Res.*, 2016, **55**, 4278–4284.
4 J. Xiong, Y. Fan and F. Luo, *Dalton Trans.*, 2020, **49**, 12536–12545.
5 C. J. Bopp, C. C. Lundstrom, T. M. Johnson, R. A. Sanford, P. E. Long and K. H. Williams, *Environ. Sci. Technol.*, 2010, **44**, 5927–5933.
6 J.-i. Kakehi, E. Kamio, R. Takagi and H. Matsuyama, *Ind. Eng. Chem. Res.*, 2015, **54**, 8782–8788.

7 A. C. Sather, O. B. Berryman and J. Rebek, *J. Am. Chem. Soc.*, 2010, **132**, 13572–13574.
8 Y. K. Agrawal, P. Shrivastav and S. K. Menon, *Sep. Purif. Technol.*, 2000, **20**, 177–183.
9 R. Ganesh, K. G. Robinson, L. Chu, D. Kucsmas and G. D. Reed, *Water Res.*, 1999, **33**, 3447–3458.
10 I. Tabushi, Y. Kobuke and T. Nishiya, *Nature*, 1979, **280**, 665–666.
11 J. Wang and S. Zhuang, *Rev. Environ. Sci. Bio/Technol.*, 2019, **18**, 437–452.
12 H. Yan, J. Bai, X. Chen, J. Wang, H. Zhang, Q. Liu, M. Zhang and L. Liu, *RSC Adv.*, 2013, **3**, 23278–23289.
13 T. P. Rao, P. Metilda and J. M. Gladis, *Talanta*, 2006, **68**, 1047–1064.
14 A. Mellah, S. Chegrouche and M. Barkat, *J. Colloid Interface Sci.*, 2006, **296**, 434–441.
15 X. Shuibo, Z. Chun, Z. Xinghuo, Y. Jing, Z. Xiaojian and W. Jingsong, *J. Environ. Radioact.*, 2009, **100**, 162–166.
16 D. Fungaro, M. Yamaura and G. Craesmeyer, *International Review of Chemical Engineering (IRECHE)*, 2012, vol. 4.
17 G. Tian, J. Geng, Y. Jin, C. Wang, S. Li, Z. Chen, H. Wang, Y. Zhao and S. Li, *J. Hazard. Mater.*, 2011, **190**, 442–450.
18 P. Michard, E. Guibal, T. Vincent and P. Le Cloirec, *Microporous Mater.*, 1996, **5**, 309–324.
19 Z. Ju, E.-S. M. El-Sayed and D. Yuan, *Dalton Trans.*, 2020, **49**, 16617–16622.
20 J. Yang, H. Wang, J. Liu, M. Ding, X. Xie, X. Yang, Y. Peng, S. Zhou, R. Ouyang and Y. Miao, *RSC Adv.*, 2021, **11**, 3241–3263.
21 J. Liu, P. K. Thallapally, B. P. McGrail, D. R. Brown and J. Liu, *Chem. Soc. Rev.*, 2012, **41**, 2308–2322.
22 B. Panella and M. Hirscher, *Adv. Mater.*, 2005, **17**, 538–541.
23 B. Panella, M. Hirscher, H. Pütter and U. Müller, *Adv. Funct. Mater.*, 2006, **16**, 520–524.
24 A. Corma, H. García and F. X. Llabrés i Xamena, *Chem. Rev.*, 2010, **110**, 4606–4655.
25 A. Henschel, K. Gedrich, R. Kraehnert and S. Kaskel, *Chem. Commun.*, 2008, 4192–4194.
26 H. A. Habib, J. Sanchiz and C. Janiak, *Dalton Trans.*, 2008, 1734–1744, DOI: 10.1039/B715812B.
27 R. C. Huxford, J. Della Rocca and W. Lin, *Curr. Opin. Chem. Biol.*, 2010, **14**, 262–268.
28 Y. Zhang, Z. Jiang, J. Song, J. Song, F. Pan, P. Zhang and X. Cao, *Ind. Eng. Chem. Res.*, 2019, **58**, 16911–16921.
29 Q. Fang, G. Zhu, M. Xue, J. Sun, G. Tian, G. Wu and S. Qiu, *Dalton Trans.*, 2004, 2202–2207.
30 G. J. Halder, C. J. Kepert, B. Moubaraki, K. S. Murray and J. D. Cashion, *Science*, 2002, **298**, 1762.
31 L. E. Kreno, K. Leong, O. K. Farha, M. Allendorf, R. P. Van Duyne and J. T. Hupp, *Chem. Rev.*, 2012, **112**, 1105–1125.
32 S. Zhang, Z. Wang, H. Zhang, Y. Cao, Y. Sun, Y. Chen, C. Huang and X. Yu, *Inorg. Chim. Acta*, 2007, **360**, 2704–2710.
33 S. M. Cohen, *Chem. Rev.*, 2012, **112**, 970–1000.
34 M. Kalaj and S. M. Cohen, *ACS Cent. Sci.*, 2020, **6**, 1046–1057.
35 Z. Yin, S. Wan, J. Yang, M. Kurmoo and M.-H. Zeng, *Coord. Chem. Rev.*, 2019, **378**, 500–512.
36 Z. Wang and S. M. Cohen, *Angew. Chem., Int. Ed.*, 2008, **47**, 4699–4702.
37 Z. Wang and S. M. Cohen, *Chem. Soc. Rev.*, 2009, **38**, 1315–1329.
38 R. J. Marshall and R. S. Forgan, *Eur. J. Inorg. Chem.*, 2016, **2016**, 4310–4331.
39 J. Čejka, *Angew. Chem., Int. Ed.*, 2012, **51**, 4782–4783.
40 W. Liu, L. Zhang, F. Chen, H. Wang, Q. Wang and K. Liang, *Dalton Trans.*, 2020, **49**, 3209–3221.
41 J. Gascon, U. Aktay, M. D. Hernandez-Alonso, G. P. M. van Klink and F. Kapteijn, *J. Catal.*, 2009, **261**, 75–87.
42 S. J. Garibay and S. M. Cohen, *Chem. Commun.*, 2010, **46**, 7700–7702.
43 M. Kandiah, M. H. Nilsen, S. Usseglio, S. Jakobsen, U. Olsbye, M. Tilset, C. Larabi, E. A. Quadrelli, F. Bonino and K. P. Lillerud, *Chem. Mater.*, 2010, **22**, 6632–6640.
44 S. Sharma, S. Panja, A. Bhattacharyya, P. S. Dhami, P. M. Gandhi and S. K. Ghosh, *Dalton Trans.*, 2016, **45**, 7737–7747.
45 S. Rostamnia and H. Xin, *Appl. Organomet. Chem.*, 2014, **28**, 359–363.
46 E. Gulcay and I. Erucar, *Ind. Eng. Chem. Res.*, 2019, **58**, 3225–3237.
47 T. Isobe, Y. Arai, S. Yanagida, S. Matsushita and A. Nakajima, *Microporous Mesoporous Mater.*, 2017, **241**, 218–225.
48 M. Wang, L. Guo and D. Cao, *Sens. Actuators, B*, 2018, **256**, 839–845.
49 T. Sarita, B. Sreenivasulu, A. Suresh, C. V. S. B. Rao and N. Sivaraman, *RSC Adv.*, 2020, **10**, 14650–14661.
50 A. Kumar, A. R. Chowdhuri, A. Kumari and S. K. Sahu, *Mater. Sci. Eng. C*, 2018, **92**, 913–921.
51 S. S. Nagarkar, B. Joarder, A. K. Chaudhari, S. Mukherjee and S. K. Ghosh, *Angew. Chem., Int. Ed.*, 2013, **52**, 2881–2885.
52 H.-Y. Li, S.-N. Zhao, S.-Q. Zang and J. Li, *Chem. Soc. Rev.*, 2020, **49**, 6364–6401.
53 C. Tudisco, G. Zolubas, B. Seoane, H. R. Zafarani, M. Kazemzad, J. Gascon, P. L. Hagedoorn and L. Rassaei, *RSC Adv.*, 2016, **6**, 108051–108055.
54 C. J. Doonan, W. Morris, H. Furukawa and O. M. Yaghi, *J. Am. Chem. Soc.*, 2009, **131**, 9492–9493.
55 S. Castellanos, K. B. Sai Sankar Gupta, A. Pustovarenko, A. Dikhtiarenko, M. Nasalevich, P. Atienzar, H. García, J. Gascon and K. Freek, *Eur. J. Inorg. Chem.*, 2015, **2015**, 4648–4652.
56 X. Li, W. Ma, H. Li, Q. Zhang and H. Liu, *Coord. Chem. Rev.*, 2020, **408**, 213191.
57 M. D. Allendorf, C. A. Bauer, R. K. Bhakta and R. J. T. Houk, *Chem. Soc. Rev.*, 2009, **38**, 1330–1352.
58 C. Xiohong, Y. Sun, Y. Wang, Z. Zhang, Y. Dai, Y. Liu, Y. Wang and Y. Liu, *J. Solid State Electrochem.*, 2021, **25**, 425–433.
59 L. Li, S. Shen, J. Su, W. Ai, Y. Bai and H. Liu, *Anal. Bioanal. Chem.*, 2019, **411**, 4213–4220.